

A PHYSICAL EXPLANATION OF THE HOLLOW STRUCTURE OF WATERSPOUT TUBES

PAUL C. KANGIESER

U. S. Weather Bureau, Washington, D. C.

[Manuscript received May 14, 1954; revised June 29, 1954]

ABSTRACT

Observations of the distribution of minute foreign particles introduced into a small, mechanically produced air vortex are briefly described. Ideas that grew from these observations are developed quantitatively into a physical explanation of the hollow structure of waterspouts that depends on the balance of centrifugal and drag forces acting on condensed water particles. It is also suggested that the mechanism may operate in tornado vortices.

INTRODUCTION

The purpose of this paper is to develop a physical explanation of the hollow tubes usually observed in waterspouts. The ideas presented here grew initially from some qualitative observations made while conducting experiments with a small air vortex produced mechanically in a manner described by Dines [1]. It will be desirable to describe briefly the nature of these experiments for background purposes, even though they play little part in the physical discussion to follow.

The apparatus used in these experiments consisted of 6 screens, each of which was approximately 4 feet wide by 6 feet high and arranged as shown in the plan view of the apparatus in figure 1. The dashed square indicates an 18-inch aperture in the center of the covered top of the apparatus to which a 36-inch propeller fan was attached by means of a duct. The normal capacity of this fan is about 10,000 cubic feet of air per minute; however, its effi-

ciency was considerably reduced due to the increased static head produced by the apparatus. As the air was sucked out the top by the fan, air entering the apparatus through the two openings produced a converging air vortex approximately 8 feet in diameter and 6 feet high. If a pan of steaming water was placed on the floor in the center of the enclosure, a hollow tube of vapor closely resembling the pendant column observed in waterspouts appeared. Apparatus similar to Dines' has appeared from time to time at meteorological exhibits to demonstrate the formation of an artificial "waterspout."

EXPERIMENTAL OBSERVATIONS

In the apparatus described above, the inside radius of the hollow steam tube was approximately $\frac{1}{2}$ inch and the outside radius approximately $1\frac{1}{2}$ inch. One of the first things noticed after the experiments were begun was that if particles of a larger size than the steam particles were broadcast into the vortex, a hollow tube was formed of larger radius. For example, when water particles of the size produced by an ordinary garden insecticide spray were sprayed into the vortex a hollow tube of approximately 3 inches inside radius and 5 inches outside radius was formed; the mass of the particles from this spray was great enough with respect to the vertical velocity in that portion of the vortex that they fell to the floor where they formed an annular ring of moisture of about the dimensions mentioned. Similarly, when fine sawdust particles were broadcast into the vortex a tube of approximately 2 feet inside radius and about $2\frac{1}{2}$ feet outside radius was formed, and an annular ring of sawdust of about these dimensions was deposited on the floor of the apparatus.

PHYSICAL EXPLANATION

A well-known example of the occurrence of this phenomenon in an atmospheric vortex is found in the dust devil which Brooks [2] defines as ". . . a whirling column

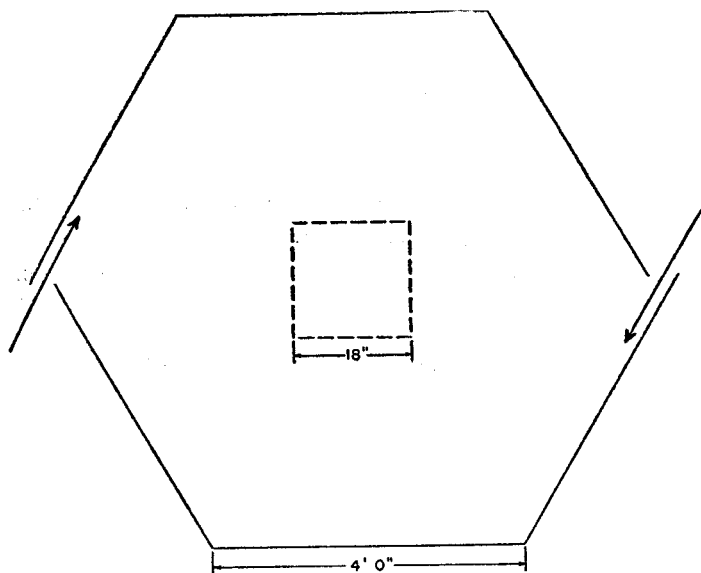


FIGURE 1.—Plan sketch of apparatus used to produce the small air vortex.

of dust or sand, in which the size of the particles increases with the distance from the center." It is proposed here that this phenomenon occurs because each foreign particle¹ introduced into the vortex seeks an equilibrium distance from the vortex axis where the inward force due to the frictional drag on the particle caused by a converging flow of air is balanced by the outward force on the particle due to centrifugal force. It should be evident that when reaching this equilibrium position, a spherical particle in a stable, non-turbulent vortex will travel in a circular path with constant velocity.

Let us begin by considering such a particle moving at constant speed in a circular path in such a vortex. The forces acting on the particle are illustrated in figure 2, where

V = velocity of the medium (air)

V_p = velocity of the particle in its path

V_d = vector difference between V and V_p

F_c = centrifugal force on the particle due to its motion

D = frictional force or "drag" produced on the particle by the motion of the medium relative to the particle

θ = angle between V and V_p .

It will be noted that the aerodynamic force on the particle caused by the wind shear in the vortex has been omitted. The order of magnitude of this force is such that it may be neglected for our purposes.

The drag force D acts in the direction of the vector expressing the velocity of the medium with respect to the particle, or along the vector V_d which expresses the vector difference between the velocity of the air and the velocity of the particle in its motion around the circular path; both V_d and D are directed toward the center of the circle of motion, and $D = F_c$.

Experiments made to determine the frictional drag of spheres in air [3] indicate that for Reynolds' numbers up to about 0.5, Stokes' formula for the frictional drag D of a sphere of diameter a , moving through an incompressible fluid of viscosity μ , with a velocity V_d with respect to the fluid, gives good agreement with the experimental values. This formula

$$D = 3\pi\mu a V_d,$$

shall be used for Reynolds' numbers up to 0.5 and experimental values of the drag coefficient [3] shall be used for Reynolds' numbers greater than 0.5.

Now for a particle of mass M

$$F_c = \frac{MV_p^2}{r},$$

where r = radius of the path. When the particle is traveling at constant speed in a circular path, $D = F_c$, or

$$3\pi\mu a V_d = \frac{MV_p^2}{r}.$$

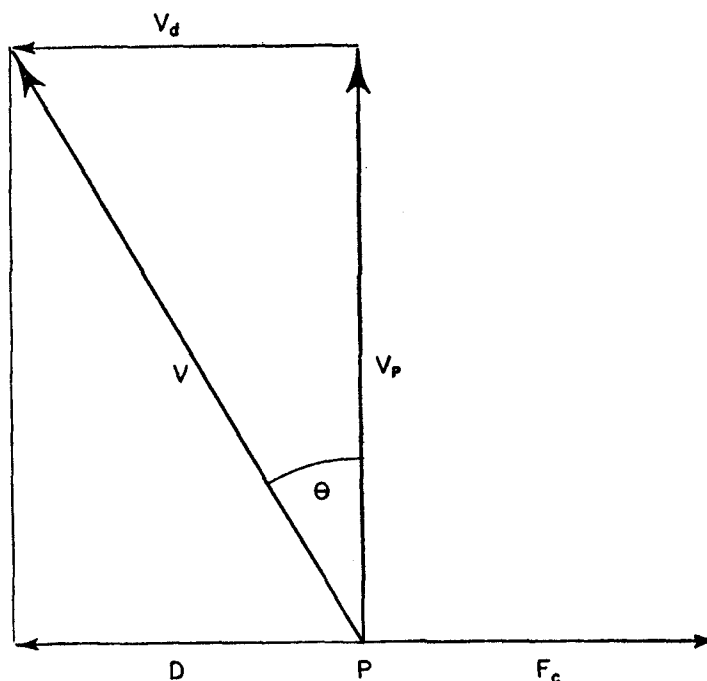


FIGURE 2.—Force and velocity diagram for a spherical particle, P , traveling at constant speed in a circular path (velocity V_p) around a vortex axis at an equilibrium distance where the inward force due to the frictional drag D on the particle caused by a converging flow of air at velocity V is balanced by the outward force on the particle due to centrifugal force F_c . The velocity of the air relative to the velocity of the particle is V_d .

The value of μ will be taken as 0.181×10^{-3} gm. cm.⁻¹ sec.⁻¹, the viscosity of dry air at 20° C. (c. g. s. units are used throughout this paper). Substituting $M = \frac{\pi\rho_p a^3}{6}$ (where ρ_p is the density of the particle) and $V_p = V_d \cot \theta$, we get

$$r = \frac{\rho_p a^2 V_d \cot^2 \theta}{18\mu}. \quad (1)$$

For Reynolds' numbers above 0.5 the general drag formula [4] will be applied using experimentally determined values for the drag coefficient

$$D = \frac{cA\rho V_d^2}{2}$$

c = drag coefficient.

A = projected area of the body in the direction of its motion relative to the fluid.

ρ = density of the fluid (for dry air at 1,000 mb. pressure, 20° C. temperature this equals 1.190×10^{-3} gm. cm.⁻³).

V_d = velocity of the body relative to the fluid.

Again, $D = F_c$ or

$$\frac{cA\rho V_d^2}{2} = \frac{MV_p^2}{r}$$

from which

$$r = \frac{4}{3} \frac{\rho_p a}{\rho c} \cot^2 \theta \quad (2)$$

¹ The word "particle" throughout this discussion will always signify a foreign particle introduced into the vortex as distinct from a parcel of air.

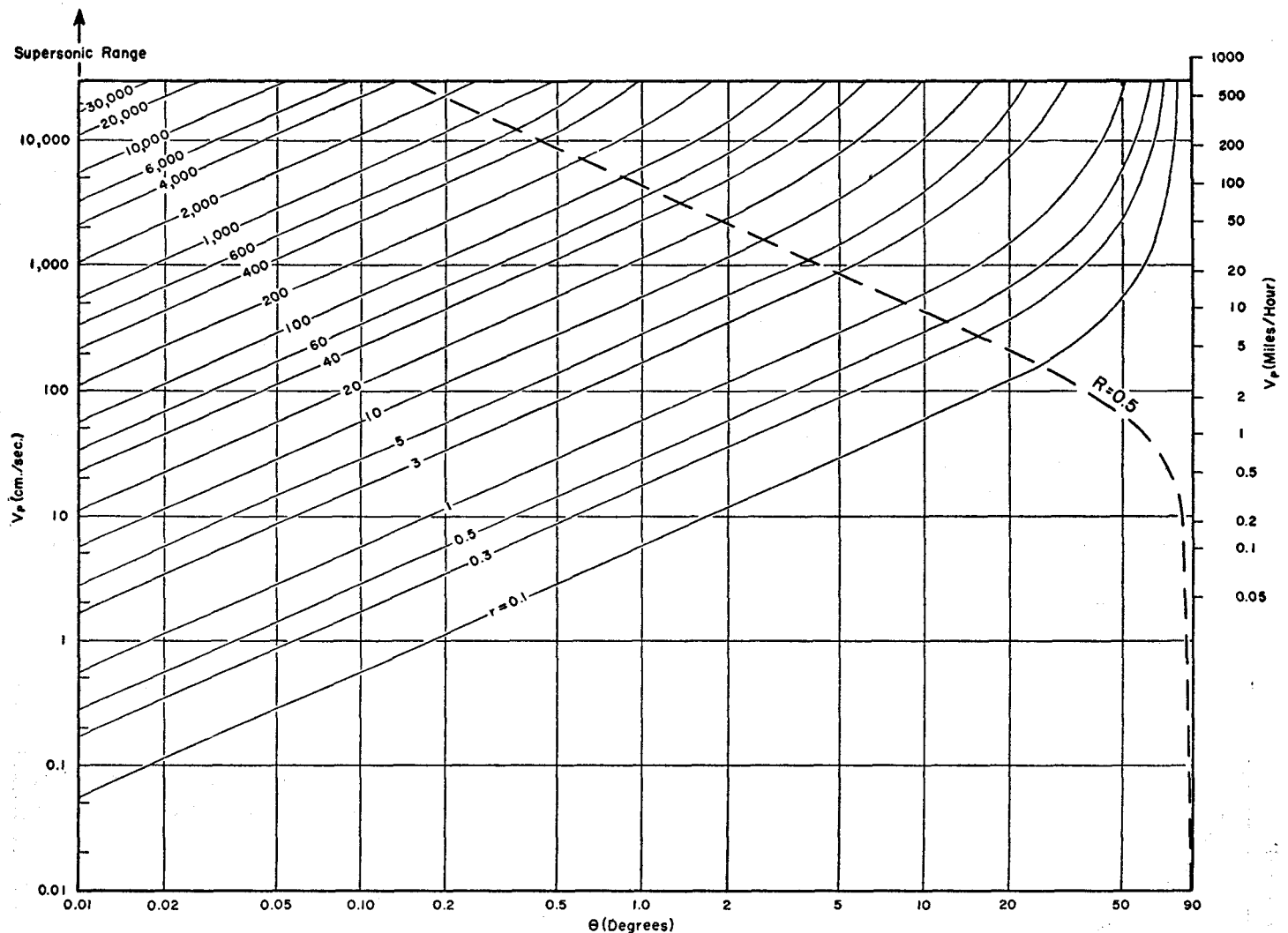


FIGURE 3.—Graph showing the relationship between V_p , r , and θ for water particle 10 microns in diameter. Stokes' law was used for Reynolds' numbers $R \leq 0.5$ (for which values of constant r define straight lines). For $R > 0.5$ experimental values for the drag coefficient (see text) were used.

Using relations (1) and (2) it is possible to construct a graph of V_p against θ and draw lines of constant r for spherical particles of a given diameter and density. Figure 3 is such a graph for spherical water particles 10 microns in diameter (about the average size of strato-cumulus cloud particles). Formula (1) yielded the straight lines to the left of the line indicating values of Reynolds' number R equal to 0.5; formula (2) gave the curved lines to the upper right. The values of r are plotted in centimeters, hence division by 30 converts them roughly into feet.

As an example of the use of the chart, let us suppose that the particles forming the inside of the visible tube in the laboratory vortex are 10 microns in diameter and that the tube is 1 centimeter in inside radius. Then if the tangential velocity of the air at that part of the vortex is 10 miles per hour, the angle θ must have a value of $7\frac{1}{2}$ degrees. The slope of the lines of constant r on the chart for constant particle velocity indicates that the value of the angle θ decreases as the radius of the hollow tube

increases. For example, to produce a hollow tube of radius greater than about 3 feet would require that the angle θ be less than about 3 degrees or V_p supersonic.

WATERSPOUTS

Photographs of waterspouts indicate that hollow tubes are usually observed. Hence, if we accept the above explanation of their occurrence, any model for such a waterspout vortex must provide for convergence in the wind field in the neighborhood of the hollow tube. As mentioned above, figure 3 indicates that there is probably less convergence within the hollow tubes of waterspouts than within the tube in the laboratory model. Another important difference is that the laboratory tube is composed of steam particles introduced into the vortex from below by the pan of steaming water, while the waterspout tube is probably composed of water particles formed near the center of the vortex by condensation due to low pressure in this region.

A model for the horizontal wind field in a waterspout vortex will now be proposed and discussed in terms of the ideas presented above. The model used will be the Rankine combined vortex which has appeared frequently in the literature; it was used by Williams [5] to describe the pressure distribution in dust devils, by Deppermann [6] in a discussion of typhoons and, most recently, by Lewis and Perkins [7] to calculate the tangential velocity distribution from the recorded pressure distribution in the outer portion of a tornado. In this model the wind follows a spiral in approaching the center with increasing speed. The entire vortex consists of two parts, an outer portion in which $V_p r = \text{constant}$, and an inner part within which solid rotation occurs and $V_p/r = \text{constant}$. The pressure in this vortex also decreases toward the center where the lowest value is reached, as shown schematically in figure 4. We will now discuss the conditions which the distribution of θ must satisfy in such a vortex for there to be (1) an equilibrium position in the outer portion, (2) an equilibrium position in the inner portion, and (3) one equilibrium position in the outer portion and one in the inner portion.

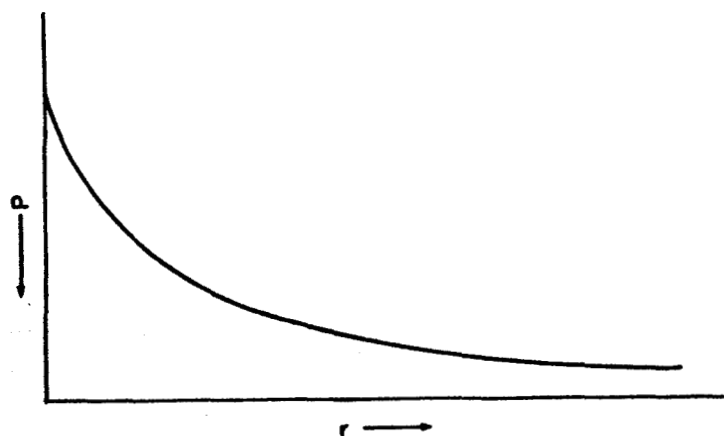


FIGURE 4.—Schematic representation of the horizontal distribution of pressure in the Rankine combined vortex discussed in the text.

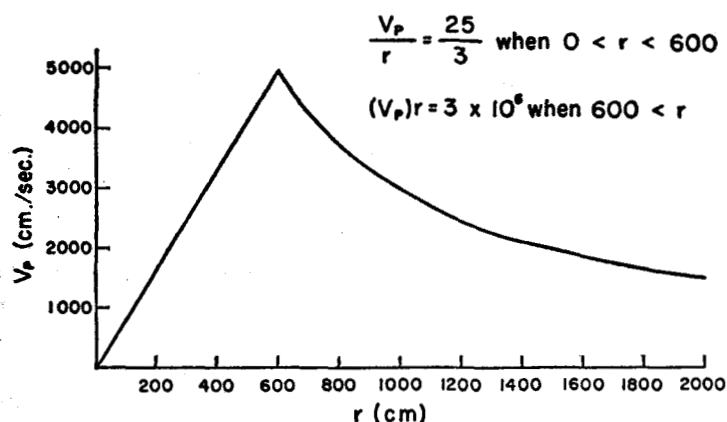


FIGURE 5.—Graph showing the horizontal distribution of tangential velocity for the Rankine combined vortex described in the text (c. g. s. units).

Given a Rankine combined vortex with the following specifications (see fig. 5)

$$V_p/r = 25/3, \text{ when } 0 < r < 600$$

$$V_p r = 3 \times 10^6, \text{ when } r > 600$$

the value of the angle θ at which a 10 micron spherical water particle will reach equilibrium is shown in figure 6 as a function of r .

(1) *An equilibrium position in the outer portion of the vortex.* Referring to figure 6, for all actual distributions of θ for which there is a region wherein the actual θ curve crosses the critical θ curve, and for which $\theta_{\text{actual}} > \theta_{\text{critical}}$ when $r > E$ and for which $\theta_{\text{actual}} < \theta_{\text{critical}}$ when $600 < r < E$, there will be an equilibrium position at the point of intersection. It should be emphasized that the dashed curve indicating the "actual θ distribution" in figure 6 is arbitrary in that the curve of actual θ may be of any degree and still satisfy the above requirements.

For purposes of illustration, let us suppose that the pressure and moisture conditions in the outer portion of a waterspout tube are such that condensation of water par-

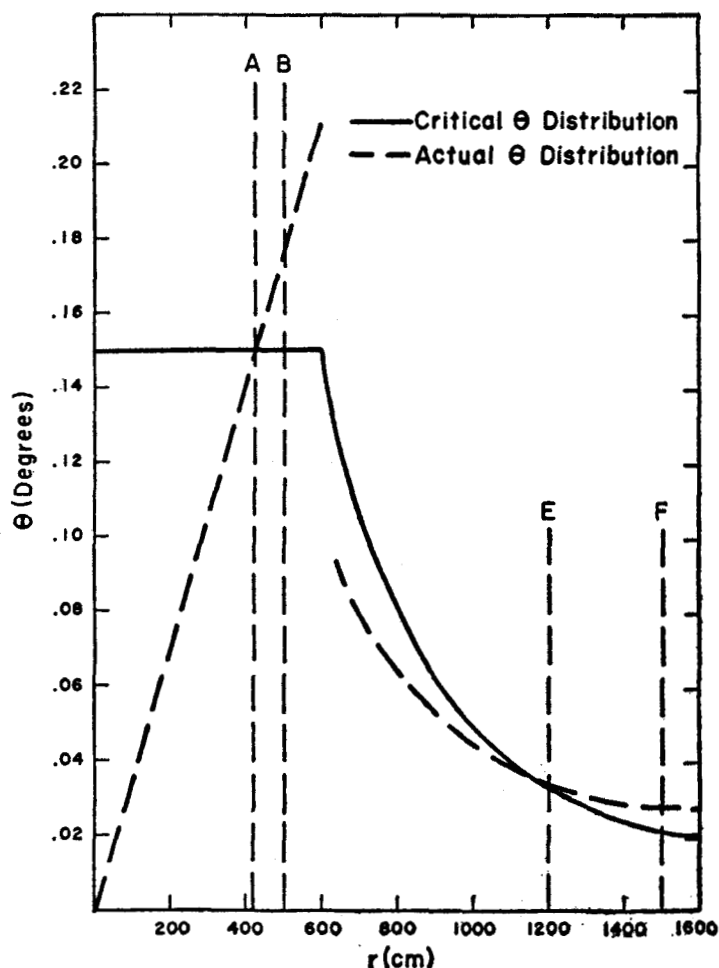


FIGURE 6.—Graph showing the value of the angle θ at which a 10 micron spherical water particle will reach equilibrium as a function of r for a vortex with the tangential velocity distribution shown in figure 5.

ticles 10 microns in diameter occurs as the converging air reaches the distance $r=F$ from the vortex axis. There will be a visible vapor tube in the region $E < r < F$ (see fig. 6), provided θ were greater than the critical values for $E < r$, and less than the critical values for $600 < r < E$. For, with the given velocity distribution, when $E < r$ the drag force on the particle exceeds the centrifugal force and the water particle is forced inward; however as soon as it passes the point E and $600 < r < E$, the centrifugal force exceeds the drag force and the particle is thrown outward, finally to travel in its equilibrium orbit at $r=E$ with constant velocity, while the air from which the particle was condensed continues to follow a spiral path inward toward the center of the vortex.

(2) *An equilibrium position in the inner portion of the vortex.* In figure 6, for all actual distributions of θ for which there is a region wherein the actual θ curve crosses the critical θ curve, and for which $\theta_{\text{actual}} > \theta_{\text{critical}}$ when $A < r < 600$, and $\theta_{\text{actual}} < \theta_{\text{critical}}$ when $0 < r < A$, there will be an equilibrium position at the point of intersection. One such distribution is shown by the heavy dashed line in figure 6. For example, if the pressure and moisture conditions in the inner portion of a waterspout tube are such that conden-

sation of water particles 10 microns in diameter occurs as the converging air reaches the distance $r=B$ from the vortex axis (fig. 6), there will be a visible vapor tube in the region $A < r < B$, provided θ is greater than the plotted critical values for $A < r < 600$ and less than the critical values for $0 < r < A$.

(3) *One equilibrium position in the outer portion and at the same time, one in the inner portion.* If pressure and moisture conditions within the vortex are such that condensation of liquid droplets of 10 microns diameter occurs within both the inner and the outer portions as soon as the converging air passes some point, say $r=F$ in figure 7, and θ has some distribution like that shown by the heavy dashed line, there will be a tendency for a concentration of particles at radii $r=A$ and $r=E$, and a sparsity of particles in the neighborhood of $r=C$, thus giving the illusion of two concentric vapor tubes. Here again the distribution of θ shown is only one of an infinite number which will satisfy the necessary conditions.

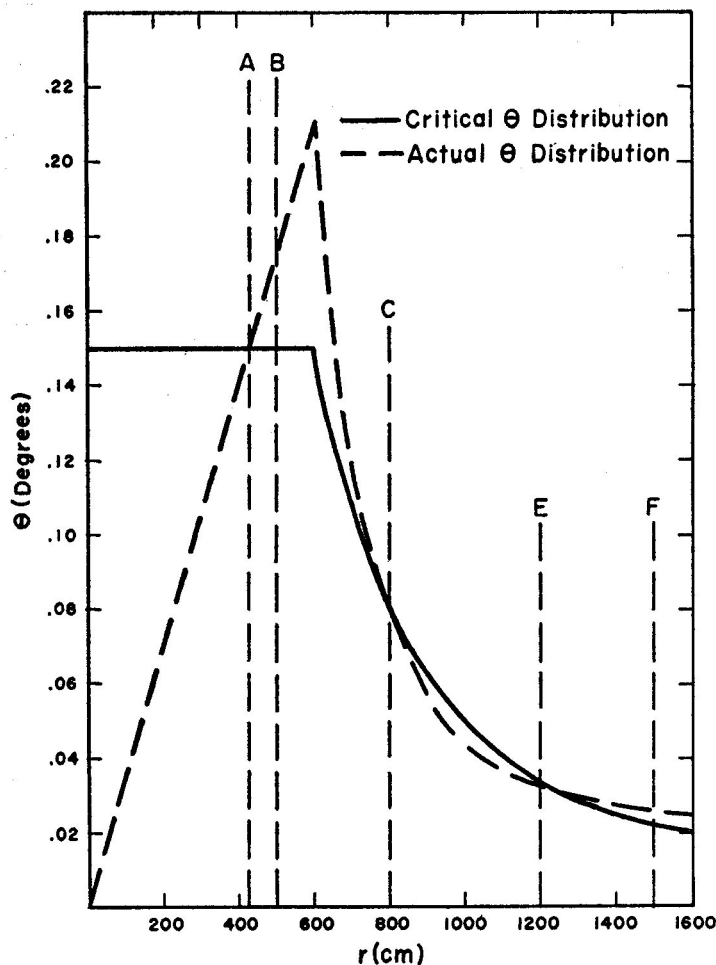


FIGURE 7.—Graph showing a possible distribution of θ which would produce one hollow tube in the inner portion and one hollow tube in the outer portion of a vortex with the tangential velocity distribution shown in figure 5.

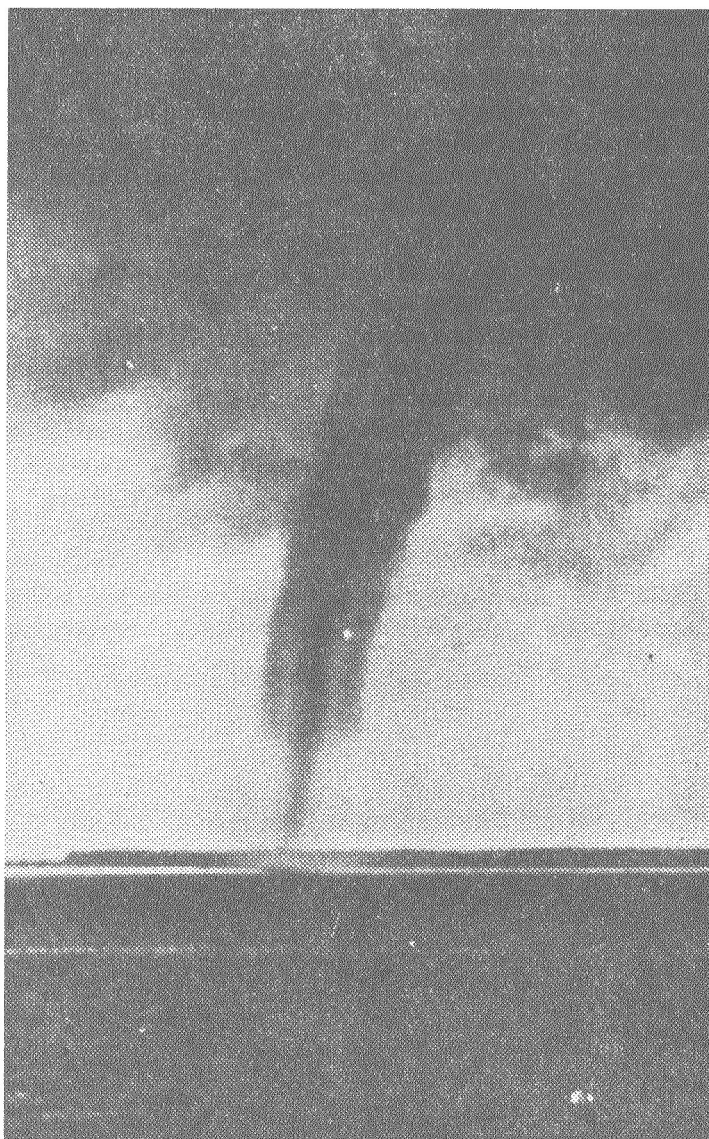


FIGURE 8.—Waterspout on the Choptank River Md., 12:20 p. m., August 28, 1938.

Inasmuch as the pressure within the inner portion of our vortex model is lower, condensation would be expected to occur there first during formation; conversely evaporation would be expected to occur first in the outer portion during dissipation. The waterspout pictured in figure 8 occurred on the Choptank River, Md., at 12:20 p. m. on August 28, 1938. The photographer submitted the following remarks with the picture: "Spout beginning to deteriorate. Notice how outside layer is already starting to retreat upward. Spout then about 10 minutes old." It should be emphasized that all of the previous remarks refer only to flow in the vortex above the friction layer. Flow near the surface in waterspout and tornado vortices is probably more much convergent, due primarily to the tendency for particles of air retarded by surface friction to conserve their angular momentum by moving toward the center of rotation.

TORNADOES

It seems reasonable to believe that the mechanism just described also operates in tornado vortices, but that the strength of these vortices is considerably greater than that of waterspouts, so that condensation in the inflowing air occurs far enough from the axis to obscure the hollow structure of the tubes. It is possible that the outside of the tornado funnel marks the outer distance from the axis at which condensation is taking place in the converging air under the existing pressure and moisture distribution in the vortex. The fact that this condensation takes place farther from the axis at higher elevations, thereby producing the characteristic funnel-shaped cloud of the tornado, may be due to one or more of the following effects: (1) higher relative humidities aloft, (2) greater vortex strength aloft, (3) the fact that slightly less lifting is required to saturate air with a given relative humidity at higher elevations.

CONCLUSIONS

The mechanism proposed above to explain the hollow tubes of waterspouts suggests that horizontal convergence

is occurring in the waterspout vortex. Inasmuch as there is evidence of the operation of the proposed mechanism in dust devils and tornadoes, it is indicated that horizontal convergence is also a feature of their vortices. Furthermore, if the theory presented here is correct, it suggests that the vertical motion in the visible portion of a waterspout or tornado is upward, not downward. It was found that a converging Rankine combined vortex could be used to explain some observed characteristics of waterspout tubes, however it should be emphasized that converging vortices of other specifications would have served equally well in that part of the discussion.

REFERENCES

1. W. H. Dines "Experiment Illustrating the Formation of the Tornado Cloud," *Quarterly Journal of the Royal Meteorological Society*, vol. XXII, No. 97, Jan. 1896, pp. 71-74.
2. Edward M. Brooks, "Tornadoes and Related Phenomena," *Compendium of Meteorology*, American Meteorological Society, Boston, 1951, pp. 673-680.
3. R. A. Castleman, "The Resistance to the Steady Motion of Small Spheres in Fluids," *NACA Technical Note No. 231*, Washington, D. C., Feb. 1926.
4. L. Prandtl and O. G. Tietjens, *Applied Hydro- and Aeromechanics*, 1st Edition, McGraw-Hill Book Co., New York and London, 1934, p. 92.
5. Nelson R. Williams, "Development of Dust Whirls and Similar Small-Scale Vortices," *Bulletin of the American Meteorological Society*, vol. 29, No. 3, Mar. 1948, pp. 106-116.
6. C. E. Deppermann, "Notes on the Origin and Structure of Philippine Typhoons," *Bulletin of the American Meteorological Society*, vol. 28, No. 9, Nov. 1947, pp. 399-404.
7. William Lewis and Porter J. Perkins, "Recorded Pressure Distribution in the Outer Portion of a Tornado Vortex," *Monthly Weather Review*, vol. 81, No. 12, Dec. 1953, pp. 379-385.